1440

Submitted to IEEE Journal of Selected Topics in Quantum Electronics

11/09/97

Miniature Erbium:Ytterbium Fiber Fabry-Perot Multiwavelength Lasers

Shinji Yamashita†, Kevin Hsu‡, and Wei H. Loh†,

†Optoelectronics Research Centre, University of Southampton

Southampton SO17 1BJ, UK

Tel: +44-1703-593139

E-mail: sy2@orc.soton.ac.uk

‡Micron Optics, Inc.

2801 Buford Highway, Suite 140, Atlanta, Georgia 30329, USA

Abstract

We demonstrate stable simultaneous lasing of up to 29 wavelengths in miniature 1mm and 2mm long Er^{3+}:Yb^{3+} fiber Fabry-Perot lasers. The wavelengths are separated by 0.8nm (100GHz) and 0.4nm (50GHz) respectively, corresponding to the free spectral range of the laser cavity. The number of lasing wavelengths

and the power stability of the individual modes are greatly enhanced by cooling the laser in liquid nitrogen (77K). The polarization modes and linewidth of each wavelength are measured with high resolution by heterodyning with a local oscillator. The homogeneous linewidth of the Er^{3+}:Yb^{3+} fiber at 77K is determined to be ~0.5nm, from spectral hole-burning measurements, which accounts for the generation of a stable multiwavelength lasing comb with wavelength separations of 0.4nm.

1. Introduction

Compact and stable multiwavelength lasers are attractive for many applications, particularly in wavelength division multiplexed (WDM) systems. Recently, multiwavelength Er^{3+}-doped fiber lasers have been reported by several groups[1]-[3], in which the doped fiber is cooled by liquid nitrogen to reduce the homogeneous linewidth and minimise cross-gain saturation effects[4]. Alternatively, inhomogeneous broadening can be achieved by the use of twin-core Er^{3+}-doped fibers[5]. In all these reports, however, the laser cavities are

at least several meters in length, and therefore tend to be unstable or multi-moded within each individual wavelength band. In addition, intracavity filters are typically needed in order to generate the comb spectrum with the desired wavelength separations.

In this paper, we report on miniature (millimeter long) Er^{3+}:Yb^{3+} fiber Fabry-Perot lasers as potentially attractive multiwavelength sources, since they are compact, inherently simple in design, and would be naturally single moded within each wavelength band. We demonstrate stable simultaneous lasing of up to 29 wavelengths in 1mm and 2mm long fiber lasers, whose wavelength separations are 0.8nm (100GHz) and 0.4nm (50GHz) respectively, corresponding to the free spectral range of the laser cavity. These wavelength spacings are ideally suited for dense WDM systems. We show that the number of lasing wavelengths and the output stability are greatly enhanced by cooling the laser in liquid nitrogen (77K). The polarization modes and linewidth of each wavelength are studied through high resolution heterodyne measurements. With Er^{3+}:Yb^{3+} co-doped fibers, the large 980nm pump absorption due to the Yb^{3+} enables more efficient operation, particularly in short cavity lasers. In addition, as will be shown here from spectral hole burning measurements, the homogeneous linewidth of the Er^{3+}:Yb^{3+} fibers at 77K is only $\sim$0.5nm, nar-

rower than for conventional Er^{3+}-doped fibers, enabling stable laser operation with wavelength separations of just 0.4nm.

2. Characteristics of the fiber Fabry-Perot lasers (FFPL)

The fiber Fabry-Perot laser (FFPL) configuration is shown in Fig.1. It consists simply of a short length of Er^{3+}:Yb^{3+} fiber with high reflectivity dielectric mirrors deposited on the two polished end-faces[6][7], and single mode fibers epoxied on both ends for coupling the pump and output emissions. It is pumped by a laser diode operating at 980nm. With mm long cavities, the mode spacing is on the order of several tens of GHz, ideally suited for dense WDM systems. Four FFPLs were studied in combination with two different types of Er^{3+}:Yb^{3+} fibers (phosphosilicate and phosphate) and two cavity lengths (1mm and 2mm). The phosphosilicate fiber has Er^{3+}:Yb^{3+} concentrations of 1000:12800 parts in 10^6, a cutoff wavelength of 1120nm, and an effective emission cross section of $6.8\times10^{-25}m^2$. The phosphate fiber has higher Er^{3+}:Yb^{3+} concentrations of 1600:38000 parts in 10^6, a cutoff wavelength of 1000nm, and an effective emission cross section of $5.7\times10^{-25}m^2$. 99.99% and 99.86% mirrors are deposited on the ends, with the latter used as output.

2.1 Spectral characteristics

Figures 2-5 show the lasing optical spectra for FFPL#1 (2mm phosphosilicate fiber), FFPL#2 (1mm phosphosilicate fiber), FFPL#3 (2mm phosphate fiber), and FFPL#4 (1mm phosphate fiber), respectively. At 77K with the lasers immersed in liquid nitrogen, it is seen that the lasers typically operate stably in two wavelength bands centered around 1535nm and 1543nm. The individual wavelength separations are 0.4nm (50GHz) for FFPL#1 and #3, and 0.8nm (100GHz) for FFPL#2 and #4, corresponding to the free spectral ranges of the respective laser cavities. The maximum number of lasing modes is 29, obtained in FFPL#3 (Fig.4(a)). However, lasing between 1536nm and 1540nm was not observed. This is on account of the deep gain dip of the Er^{3+}:Yb^{3+} fibers in this wavelength band, shown in the fluorescent spectra from these fibers (Fig.6), which was measured by the experimental setup in Fig.11 (see Section 3).

As seen in Figs.2-5, the number of achievable wavelengths is greater in 2mm-long FFPLs (#1 and #3) than in 1mm-long ones (#2 and #4). The reduction in the number with the shorter cavity is likely the consequence of the higher gain needed in the doped fiber in order to reach threshold, and

hence less saturation effects[3].

It is interesting to note that the lasers are actually also capable of multiwavelength operation at higher temperatures, such as at 195K (simply surrounding it with dry ice) and 290K (at room temperature), as shown in Figs.2-5. However, the number of modes is reduced and the output modal powers become less stable as the temperature increases. It is clearly seen in all lasers that the lasing modes are shifted to the longer wavelength as the temperature reduces, and FFPL#1 at 77K operates only in the longer wavelength band centered at 1544nm as shown in Fig.2(a).

From a practical point of view, FFPL#1 may be the most promising; although the number of modes is only 17, they are evenly spaced (without any gaps) and the output modal powers are also the most stable.

2.2 Output modal powers and their stability

Figures 7(a)-(c) show the output modal powers for FFPL#1 at (a) 77K, (b) 195K, and (c) 290K, and Figure 7(d) shows the total output powers at these temperatures. The total output powers have a slope efficiency of ~0.4%. A slight saturation of the output power at higher pump powers is clearly evident, especially at 77K, as shown in Fig.7(d). This saturation effect may be due to

a "bottleneck" problem in the energy transfer from Yb^{3+} ions to Er^{3+} ions as a consequence of the finite transfer time, enhanced at 77K; however, further investigation will be needed to verify this.

Figures 8(a)-(c) show the temporal change of output modal powers for FFPL#1 at (a) 77K, (b) 195K, and (c) 290K. The stability of the individual modal powers at 77K is excellent (within ±0.05dB), although they become less stable as the temperature goes up. The instabilities with higher temperatures are believed to be caused by cross gain saturation effects in the increasingly homogeneous Er^{3+}:Yb^{3+} fiber. In contrast, at 77K, the fiber gain medium is sufficiently inhomogeneous to enable stable multiwavelength laser operation.

2.3 Polarization modes and linewidth in each wavelength

The linewidth of each wavelength in Figs.2-5 is 0.1 nm, resolution limited by the optical spectrum analyzer. In order to measure the spectrum at higher resolution, we performed heterodyne detection with a tunable external cavity single frequency laser diode as the local oscillator. Figure 9 shows the heterodyne detected beat spectra of the 4th wavelength from FFPL#4. It is found to consist of two modes separated by 1.4GHz. By carefully changing the polarization state of the light from the local oscillator, one of the beat

signals is observed to be suppressed when the other reaches maximum, which indicates that the polarization states of the two modes are orthogonal.

We also investigated all the modes in the FFPLs, and observed similarly two beat signals separated by a few GHz. Thus it is found that the FFPLs actually operate in two polarization modes for each wavelength in Figs.2-5, since no polarization-selective mechanism exists in these lasers. As multiwavelength light sources for WDM systems, a polarizer would likely be needed after the FFPL to suppress one of the polarization modes. However, the lasing of two polarization modes separated by a certain frequency with equal powers means that the polarization state of the light is scrambled at that frequency, which may prove useful in multiwavelength sensing systems.

Figure 10 shows the beat spectrum of FFPL#4 obtained using the delayed self-heterodyne method. A frequency shifter of 110MHz and a delay fiber of 5km were used, with a nominal resolution of 40kHz. It should be noted that the beats of all the wavelengths are superimposed because no filtering is applied. The linewidth is estimated to be ~100kHz.

3. Determination of homogeneous linewidth of the Er^{3+}:Yb^{3+} fibers used

It has previously been shown that Er^{3+}-doped fibers exhibit inhomogeneous gain at low temperatures from spectral gain hole burning measurements[4], where, at 77K, the homogeneous linewidth (=half of hole width) was found to be ~1nm, depending on the host glass. To our knowledge, these measurements have not been performed for Er^{3+}:Yb^{3+} fibers. Therefore, we present here results of homogeneous linewidth measurements of the Er^{3+}:Yb^{3+} fibers used.

Figure 11 shows the experimental setup. The Er^{3+}:Yb^{3+} fiber is directly immersed in liquid nitrogen, and pumped at 1μm through a WDM coupler. We chose this pump wavelength because the absorption at 980nm was found to be too high to obtain enough amplified spontaneous emission (ASE). Signal light at 1.53μm is put into the Er^{3+}:Yb^{3+} fiber to burn a hole in the ASE spectrum. The counter-propagating ASE is taken out through a circulator. The advantages of using the counter-propagating ASE are that there is no need for optimizing the length of the Er^{3+}:Yb^{3+} fiber, and that the measured spectrum does not contain the signal light. In practice, however, a small

amount of the signal does remain in the spectrum, mainly from scattering in the fiber, so a polarization controller and polarizer are used to further suppress it (note that the ASE is unpolarized).

Figures 12(a)-(c) show the measured spectral holes in the (a) phosphosilicate Er^{3+}:Yb^{3+} fiber, (b) phosphate Er^{3+}:Yb^{3+} fiber, and (c) standard Al/Ge/SiO_2 Er^{3+}-doped fiber. The standard Er^{3+}-doped fiber measured for comparison is pumped at 980nm. It is seen in Figs.12(a) and (b) that the homogeneous linewidths of the phosphosilicate and phosphate Er^{3+}:Yb^{3+} fibers are both ~0.5nm, narrower than that for the standard Er^{3+}-doped fiber (~0.8nm) as seen in Fig.12(c). These results account for the stable multiwavelength lasing, even for wavelength separations of only 0.4nm in 2mm-long FFPLs. We also measured the spectrum at 195K and 290K, but could not observe any substantial hole-burning. At these higher temperatures, we attribute the multiwavelength operation, in spite of the homogeneous nature of Er^{3+}:Yb^{3+} fibers, to spatial hole-burning effect caused by the standing wave formed in the Fabry-Perot cavity[8].

4. Conclusion

We have reported on the realization of miniature Er^{3+}:Yb^{3+} fiber Fabry-Perot lasers (FFPL) as potentially attractive multiwavelength sources, since they are compact, inherently simple in design and construction, and would be naturally single moded within each wavelength band. We have demonstrated stable simultaneous lasing of up to 29 wavelengths in 1mm and 2mm long FFPLs, whose wavelength separations are 0.8nm (100GHz) and 0.4nm (50GHz) respectively, corresponding to the free spectral range of the laser cavity. These wavelength spacings are ideally suited for dense WDM systems. We have shown that the number of the lasing wavelengths and the output power stability are greatly enhanced by cooling the laser in liquid nitrogen (77K). The polarization modes and linewidth of each wavelength were studied with the aid of heterodyne measurements. The homogeneous linewidth of the Er^{3+}:Yb^{3+} fibers at 77K is found to be $\sim$0.5nm from spectral hole-burning measurements, thus enabling stable multiwavelength laser operation with wavelength spacings of just 0.4nm.

Acknowledgement

One of the author (S. Yamashita) acknowledges the Japan Society of the Promotion of Science (JSPS) for the postdoctoral fellowship for research abroad. The Optoelectronics Research Centre is an Interdisciplinary Research Centre funded by the UK Engineering and Physical Sciences Research Council.

References

[1] J. Chow, G. Town, B. Eggleton, M. Ibsen, K. Sudgen, and I. Bennion, "Multiwavelength generation in an erbium-doped fiber laser using in-fiber comb filters," *IEEE Photon. Technol. Lett.*, vol.8, no.1, pp.60-62, Jan. 1996.

[2] S. Yamashita and K. Hotate, "Multiwavelength erbium-doped fiber laser using intracavity etalon and cooled by liquid nitrogen," *IEE Electron. Lett.*, vol.32, no.14, pp.1298-1299, July 1996.

[3] N. Park and P. F. Wysocki, "24-line multiwavelength operation of erbium-doped fiber-ring laser," *IEEE Photon. Technol. Lett.*, vol.8, no.11, pp.1459-1461, Nov. 1996.

[4] E. Desurvire, J. L. Zyskind, and J. R. Simpson,, "Spectral gain hole-burning at 1.53μm in erbium-doped fiber amplifiers," *IEEE Photon. Technol. Lett.*, vol.2, no.4, pp.246-248, Apr. 1990.

[5] O. Graydon, W. H. Loh, R. L. Laming, and L. Dong, "Triple-frequency operation of an Er-doped twincore fiber loop laser," *IEEE Photon. Technol. Lett.*, vol.8, no.1, pp.63-65, Jan. 1996.

[6] K. Hsu, C. M. Miller, J. T. Kringlebotn, E. M. Taylor, J. Townsend, and D. N. Payne, "Single-mode tunable erbium:ytterbium fiber Fabry-Perot microlaser," *Opt. Lett.*, vol.19, no.12, pp.886-888, June 1994.

[7] K. Hsu, C. M. Miller, J. T. Kringlebotn, and D. N. Payne, "Continuous and discrete wavelength tuning in Er:Yb fiber Fabry-Perot lasers," *Opt. Lett.*, vol.20, no.4, pp.377-379, Feb. 1995.

[8] A. E. Siegman, *Lasers*, University Science, Mill Valley, Calif., 1986.

Figure Captions

Figure 1 Miniature Er^{3+}:Yb^{3+} fiber Fabry-Perot laser: experimental configuration.

Figure 2 Output optical spectra of FFPL#1 (2mm phosphosilicate Er^{3+}:Yb^{3+} fiber),
(a) 77K (b) 195K (c) 290K (Resolution: 0.1nm)

Figure 3 Output optical spectra of FFPL#2 (1mm phosphosilicate Er^{3+}:Yb^{3+} fiber),
(a) 77K (b) 195K (c) 290K (Resolution: 0.1nm)

Figure 4 Output optical spectra of FFPL#3 (2mm phosphate Er^{3+}:Yb^{3+} fiber),
(a) 77K (b) 195K (c) 290K (Resolution: 0.1nm)

Figure 5 Output optical spectra of FFPL#4 (1mm phosphate Er^{3+}:Yb^{3+} fiber),
(a) 77K (b) 195K (c) 290K (Resolution: 0.1nm)

Figure 6 Fluorescent spectra from (a) phosphosilicate Er^{3+}:Yb^{3+} fiber, and (b) phosphate Er^{3+}:Yb^{3+} fiber, at 77K pumped at 1μm. (Resolution: 0.1nm)

Figure 7 Individual modal powers of FFPL#1.
(a) 77K (b) 195K (c) 290K (d) Total power
(numbered beginning with the shortest lasing wavelength.)

Figure 8 Individual modal stabilities of FFPL#1.
(a) 77K (b) 195K (c) 290K

Figure 9 Heterodyne beat spectra of the 4th mode of FFPL#4.

Figure 10 Delayed-self heterodyne beat spectra of FFPL#4.

Figure 11 Experimental setup for spectral hole burning measurements.

Figure 12 Measured spectral holes. (Resolution: 0.1nm)
(a) phosphosilicate Er^{3+}:Yb^{3+} fiber
(b) phosphate Er^{3+}:Yb^{3+} fiber
(c) standard Al/Ge/SiO_2 Er^{3+}-doped fiber

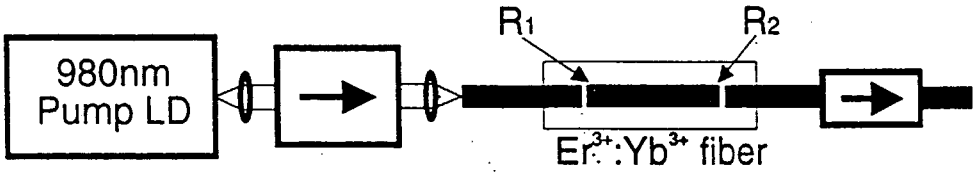

Figure 1

S. Yamashita, et al.

(a)

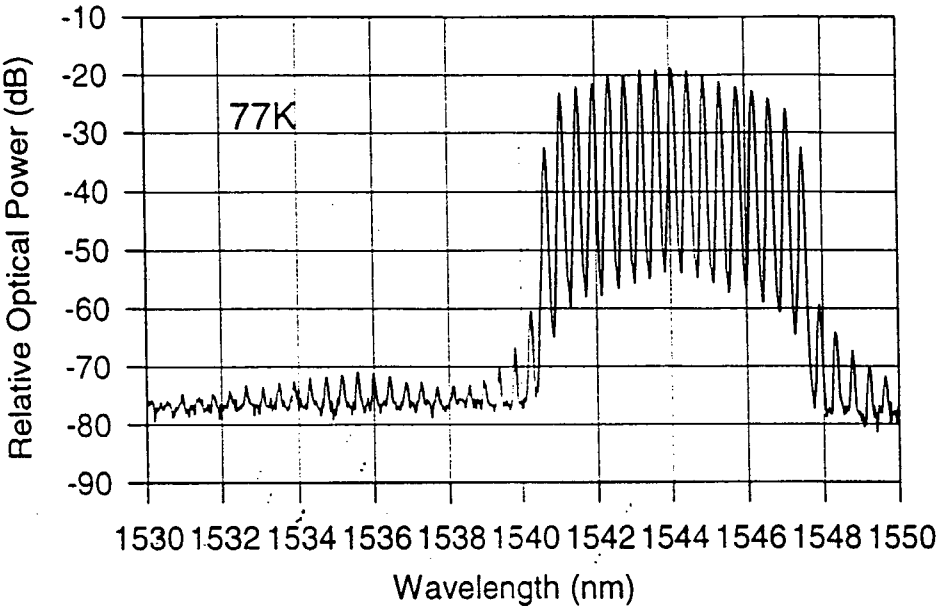

(b)

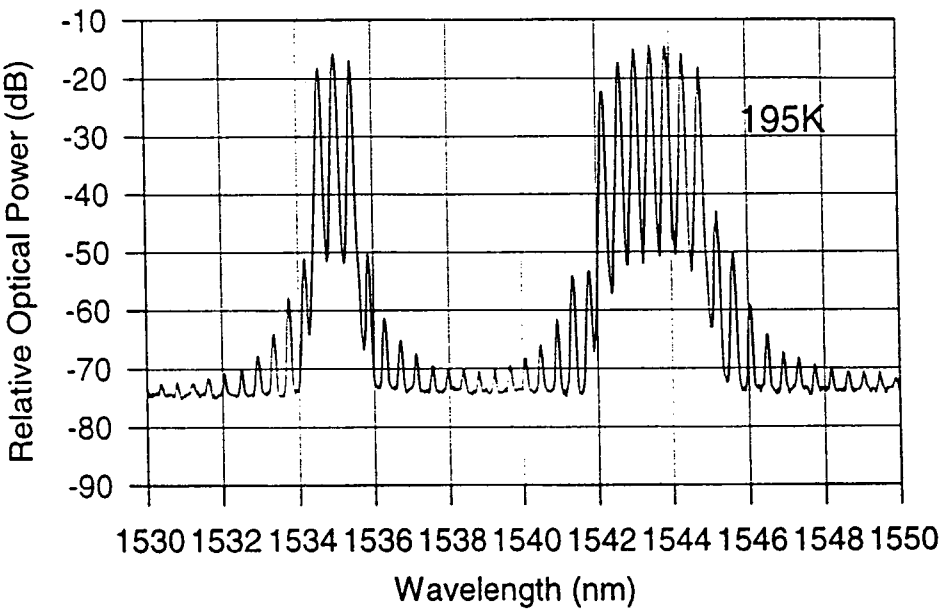

(c)

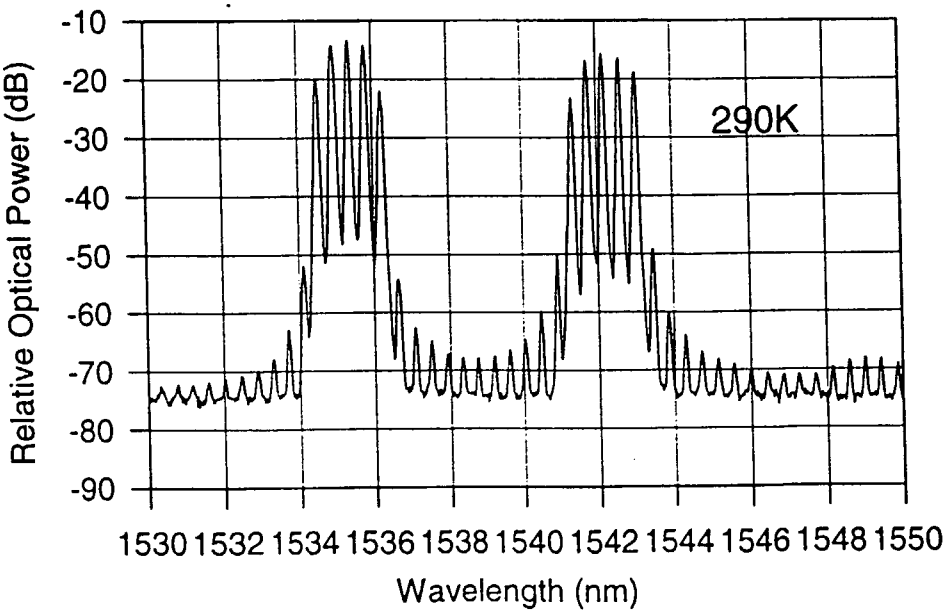

Figure 2

S. Yamashita, et al

(a)

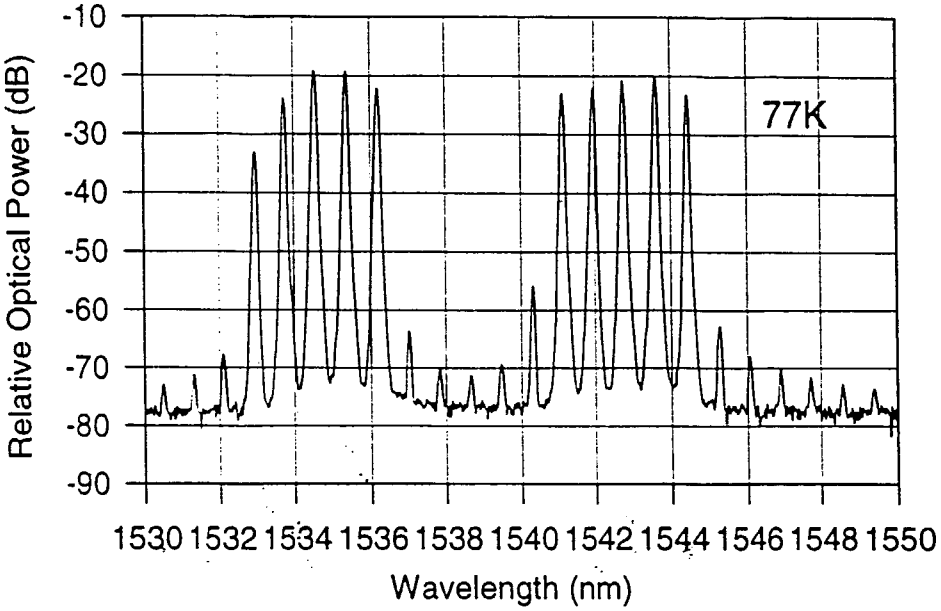

(b)

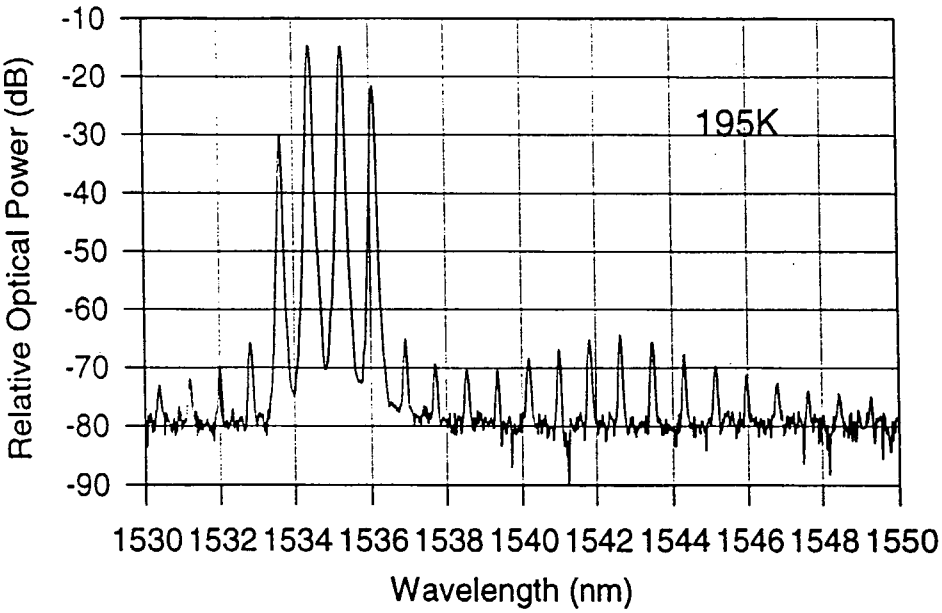

(c)

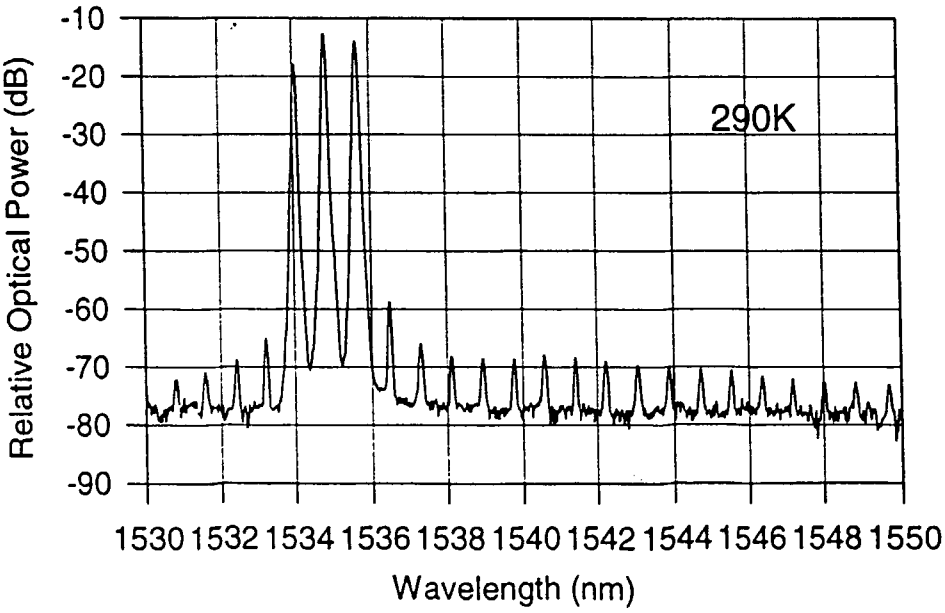

Figure 3

(a)

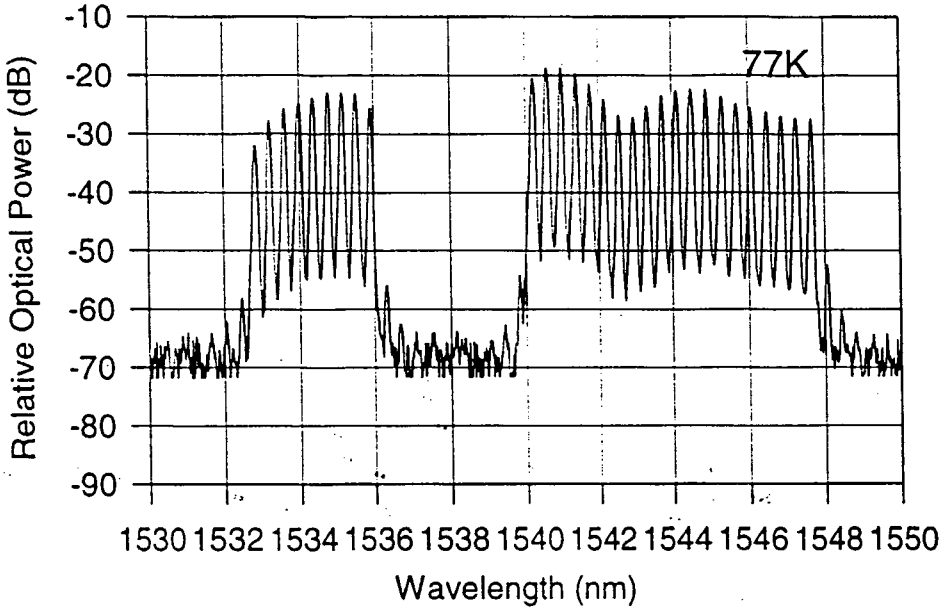
77K
Relative Optical Power (dB)
-10
-20
-30
-40
-50
-60
-70
-80
-90
1530 1532 1534 1536 1538 1540 1542 1544 1546 1548 1550
Wavelength (nm)

(b)

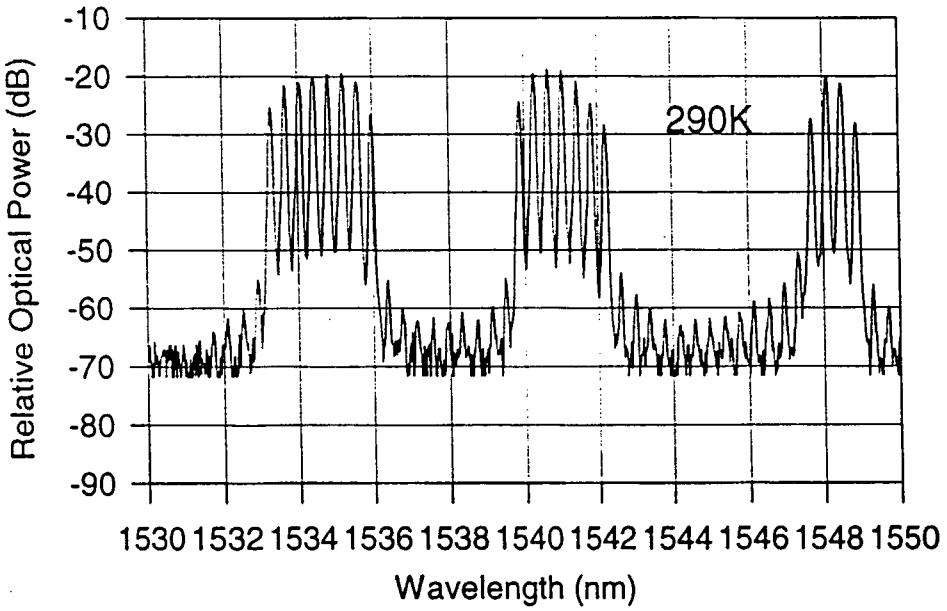
290K
Relative Optical Power (dB)
-10
-20
-30
-40
-50
-60
-70
-80
-90
1530 1532 1534 1536 1538 1540 1542 1544 1546 1548 1550
Wavelength (nm)

Figure 4

(a)

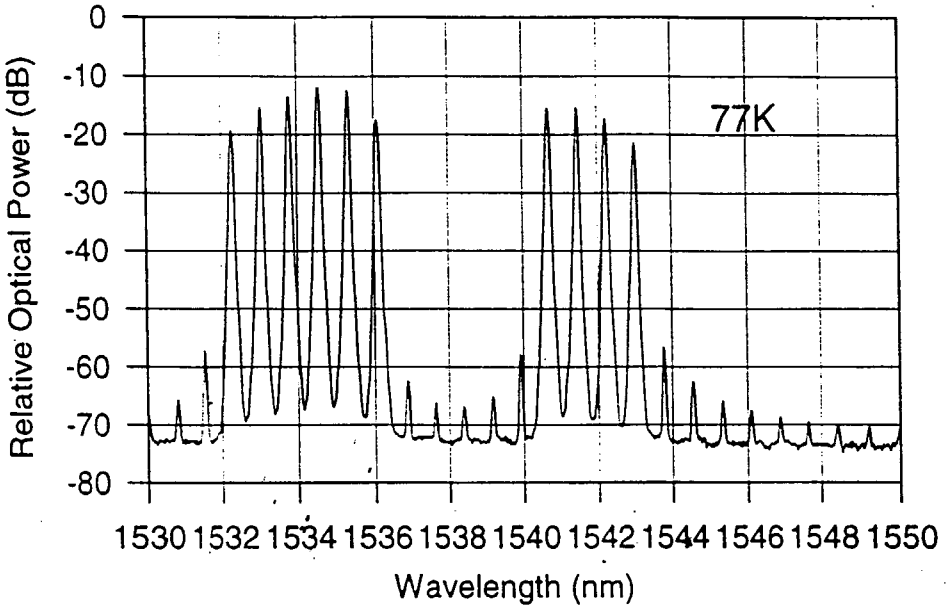
0
-10
-20
-30
-40
-50
-60
-70
-80
Relative Optical Power (dB)
77K
1530 1532 1534 1536 1538 1540 1542 1544 1546 1548 1550
Wavelength (nm)

(b)

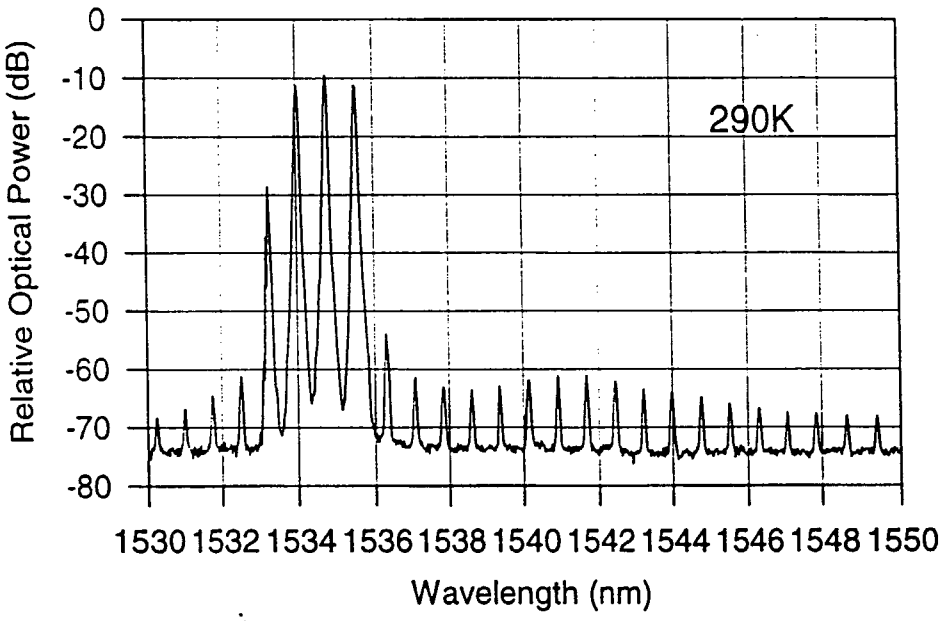
0
-10
-20
-30
-40
-50
-60
-70
-80
Relative Optical Power (dB)
290K
1530 1532 1534 1536 1538 1540 1542 1544 1546 1548 1550
Wavelength (nm)

Figure 5

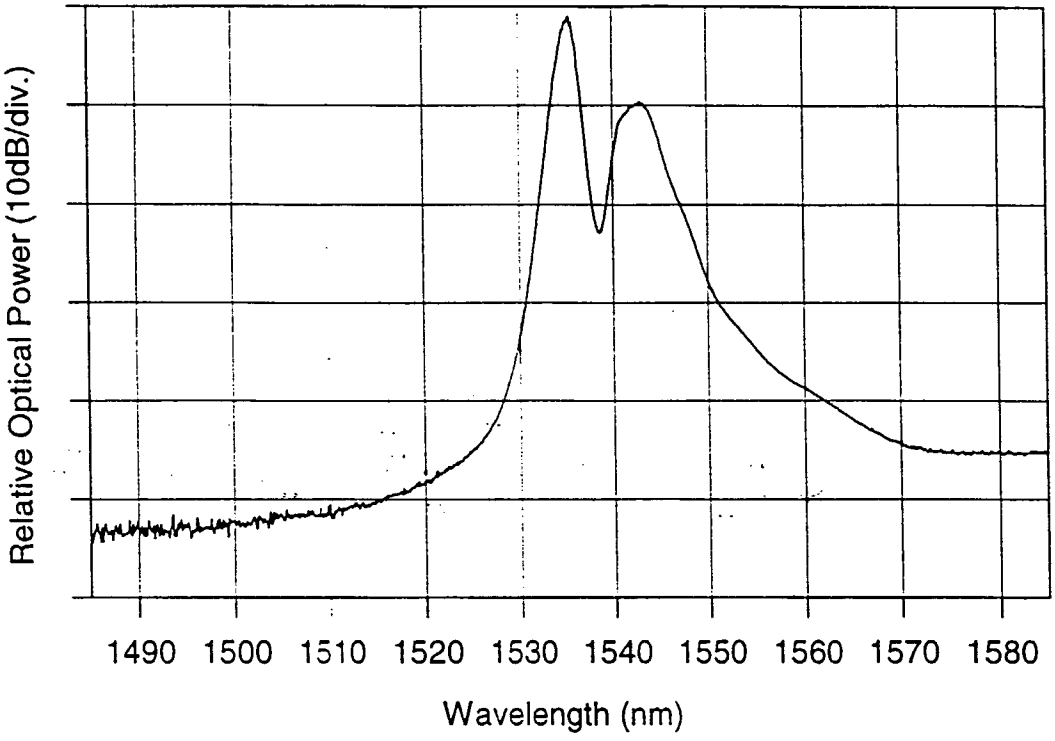
Relative Optical Power (10dB/div.)
1490 1500 1510 1520 1530 1540 1550 1560 1570 1580
Wavelength (nm)

(a)

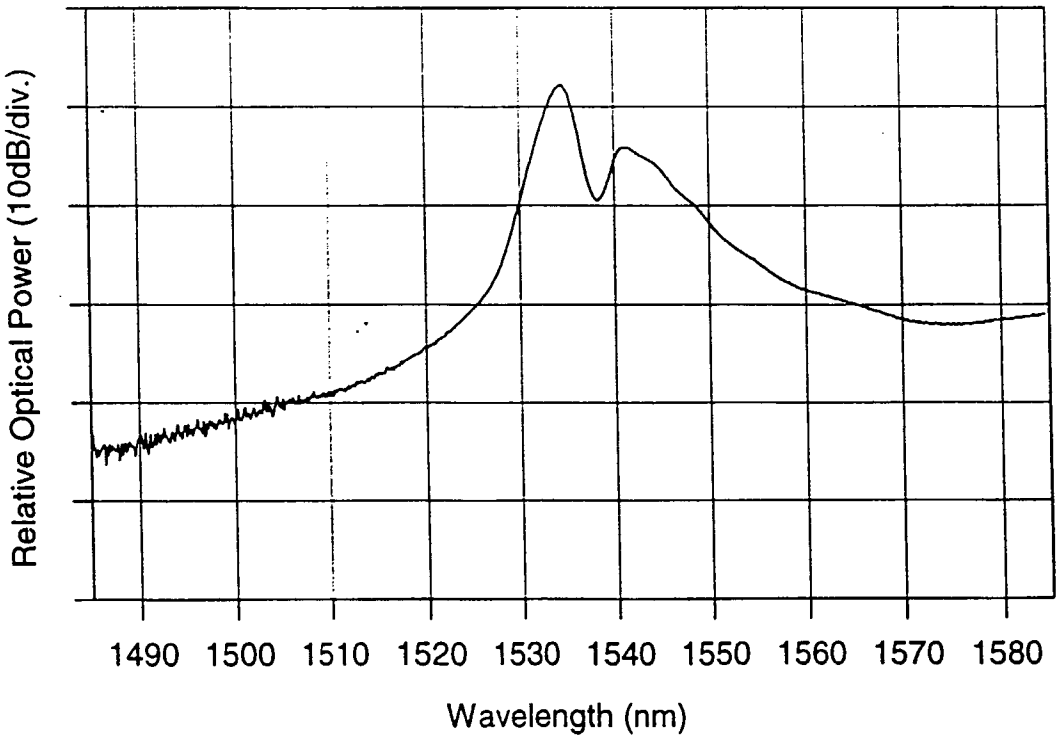
Relative Optical Power (10dB/div.)
1490 1500 1510 1520 1530 1540 1550 1560 1570 1580
Wavelength (nm)

(b)

Figure. 6

S. Kawashita, et al

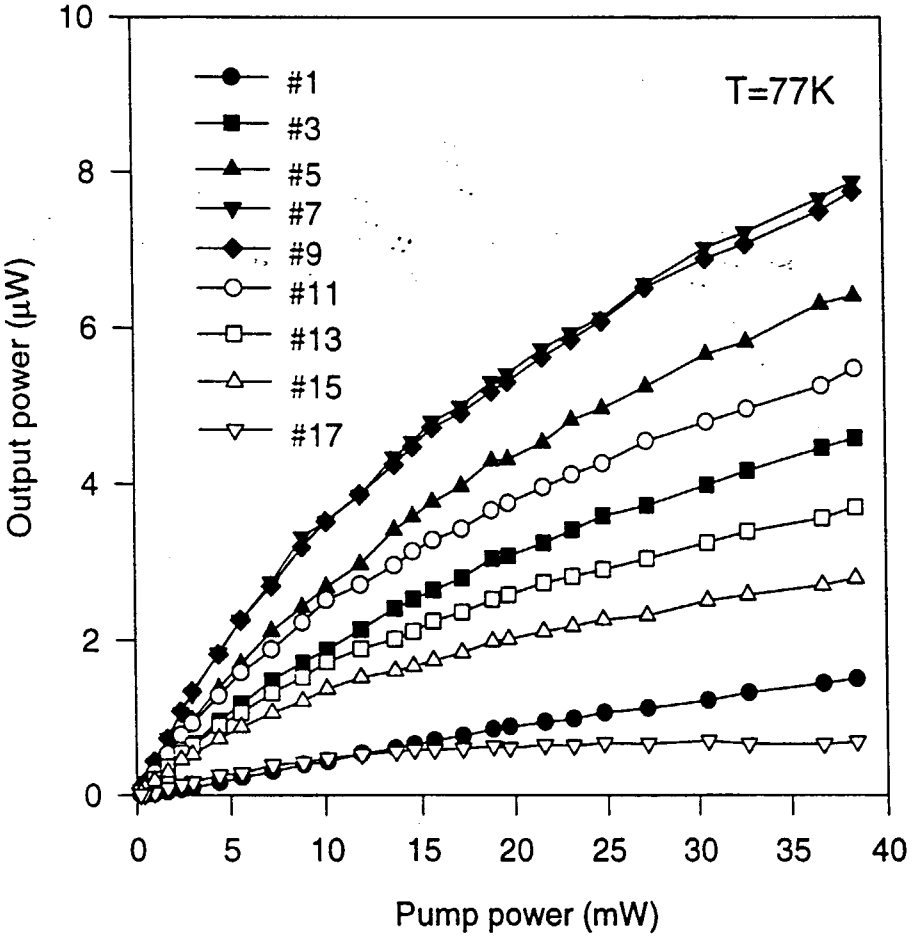

Figure 7 (a)

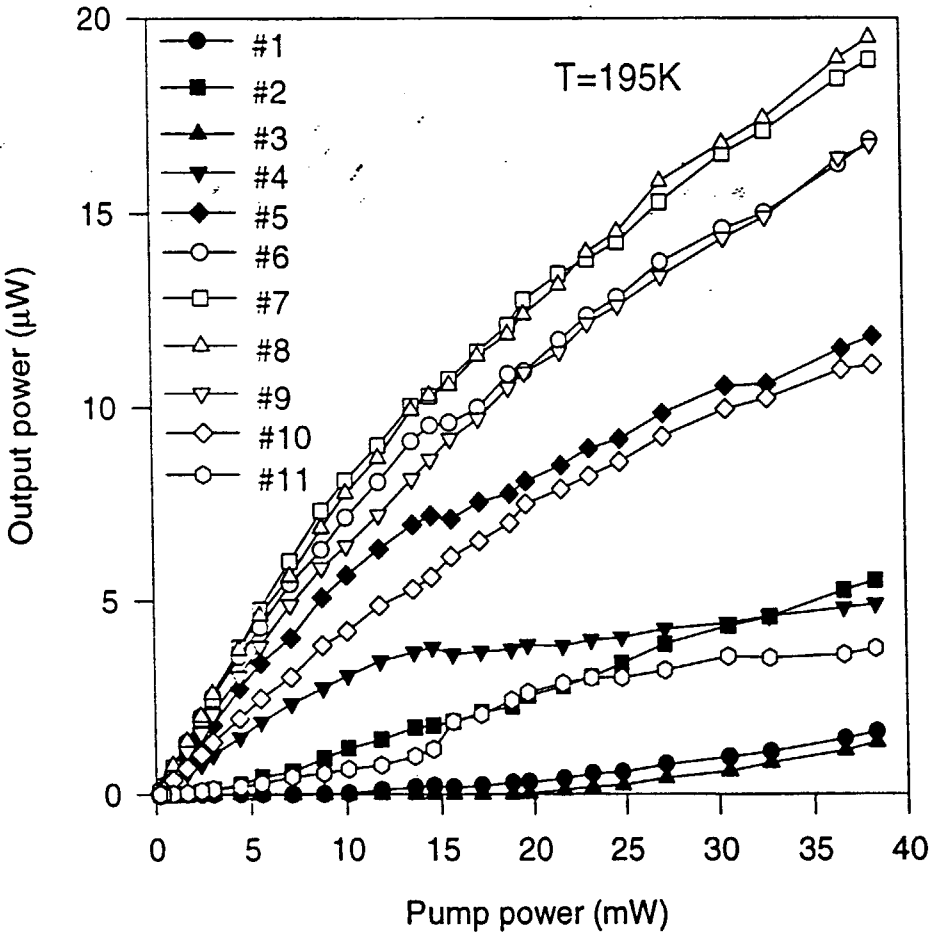
T=195K
#1
#2
#3
#4
#5
#6
#7
#8
#9
#10
#11
Output power (μW)
Pump power (mW)
0
5
10
15
20
25
30
35
40

Figure 7(b)

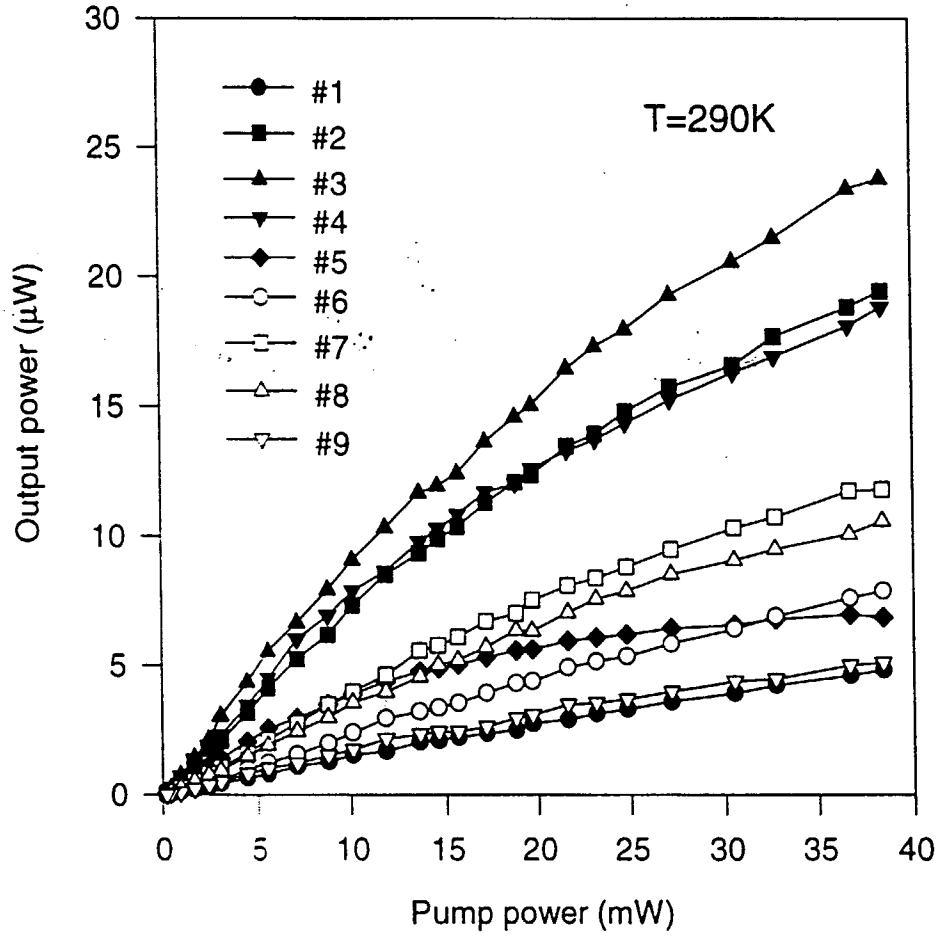
T=290K
#1
#2
#3
#4
#5
#6
#7
#8
#9
Output power (μW)
Pump power (mW)
0
5
10
15
20
25
30
35
40

Figure 7(c)

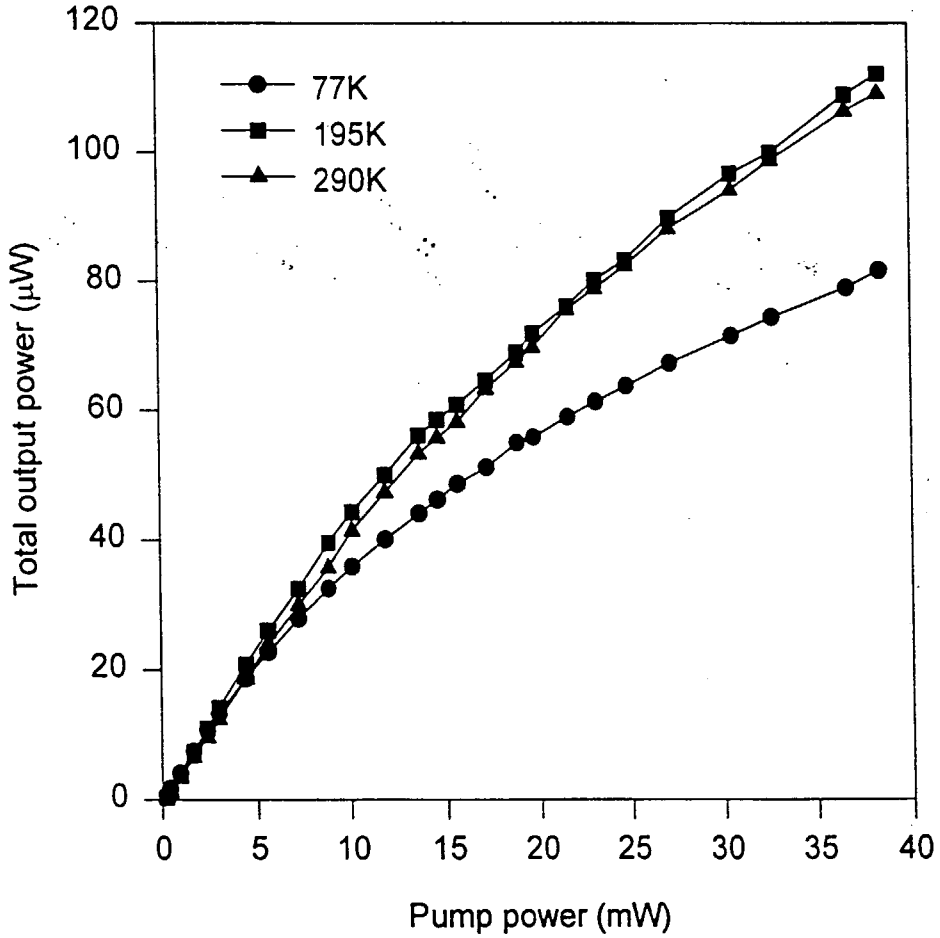
120
100
80
60
40
20
0
77K
195K
290K
Total output power (μW)
0
5
10
15
20
25
30
35
40
Pump power (mW)

Figure 7(a)

S. Yamashita, et al

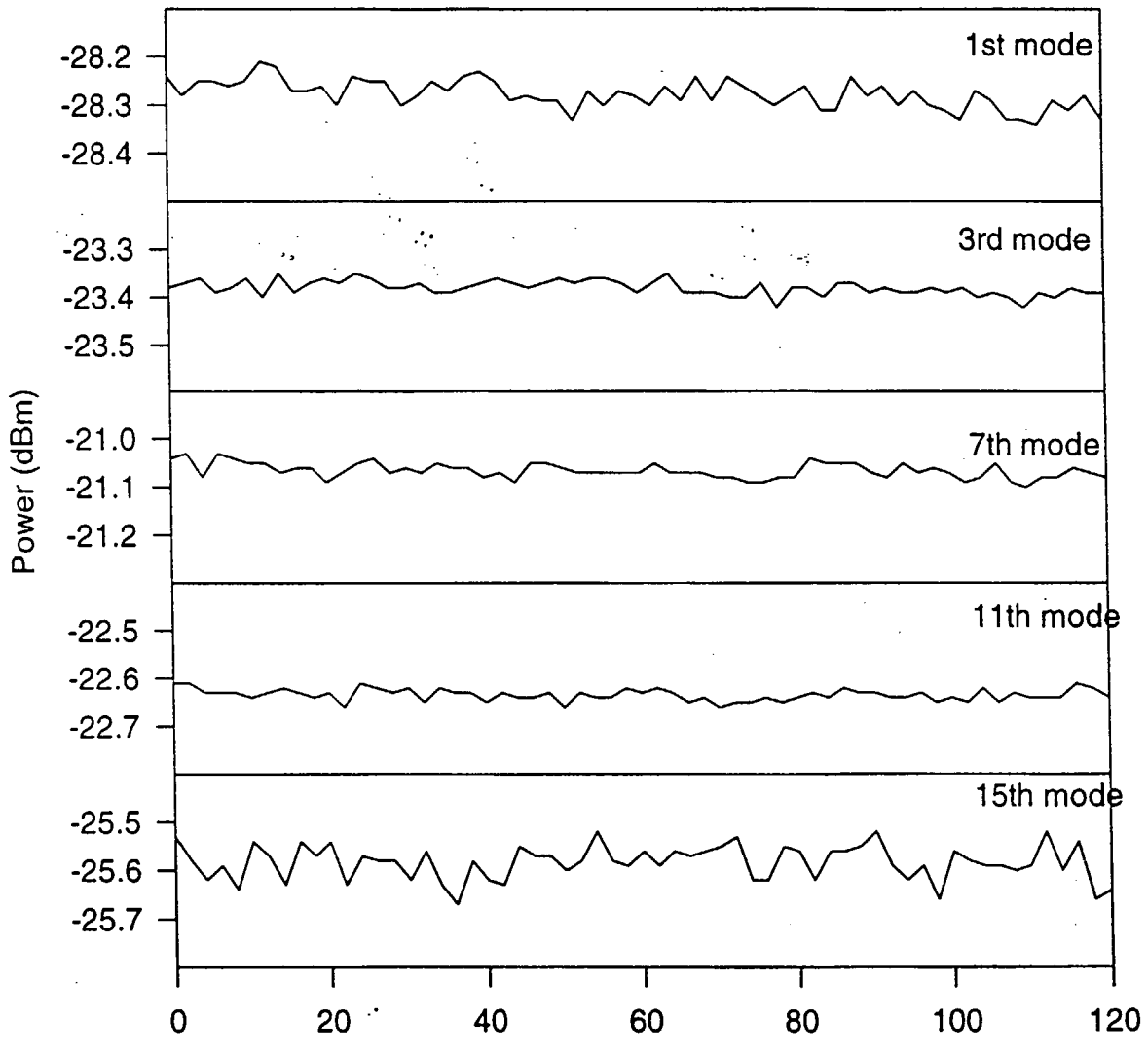


```
09-05-97  02:29p
Free: 13,369,344

 Directory Z:\USER\ACT\JSTQE\*.*

.            <DIR>          .
..           <DIR>          ..
262R1          5,059 02-05-97 02:07p   262R2          5,137 02-05-97 01:36p
262STATU.      5,277 02-05-97 02:08p   264REVI.       4,916 07-05-97 12:55p
264STATU.      5,081 07-05-97 12:51p   266REVIE.      4,924 07-05-97 12:47p
266STATU.      5,195 07-05-97 12:44p   271REVI.       4,903 07-05-97 01:20p
271REV2 .      4,974 08-05-97 03:10p   271STATU.      5,348 08-05-97 02:26p
279REV1 .      5,130 07-05-97 01:21p   279REV2 .      4,905 09-05-97 02:26p
279STATU.      5,250 09-05-97 02:26p   REVIEW .       4,935 02-05-97 01:07p
STATUS  .      4,865 07-05-97 12:40p
```

Figure 3(a)

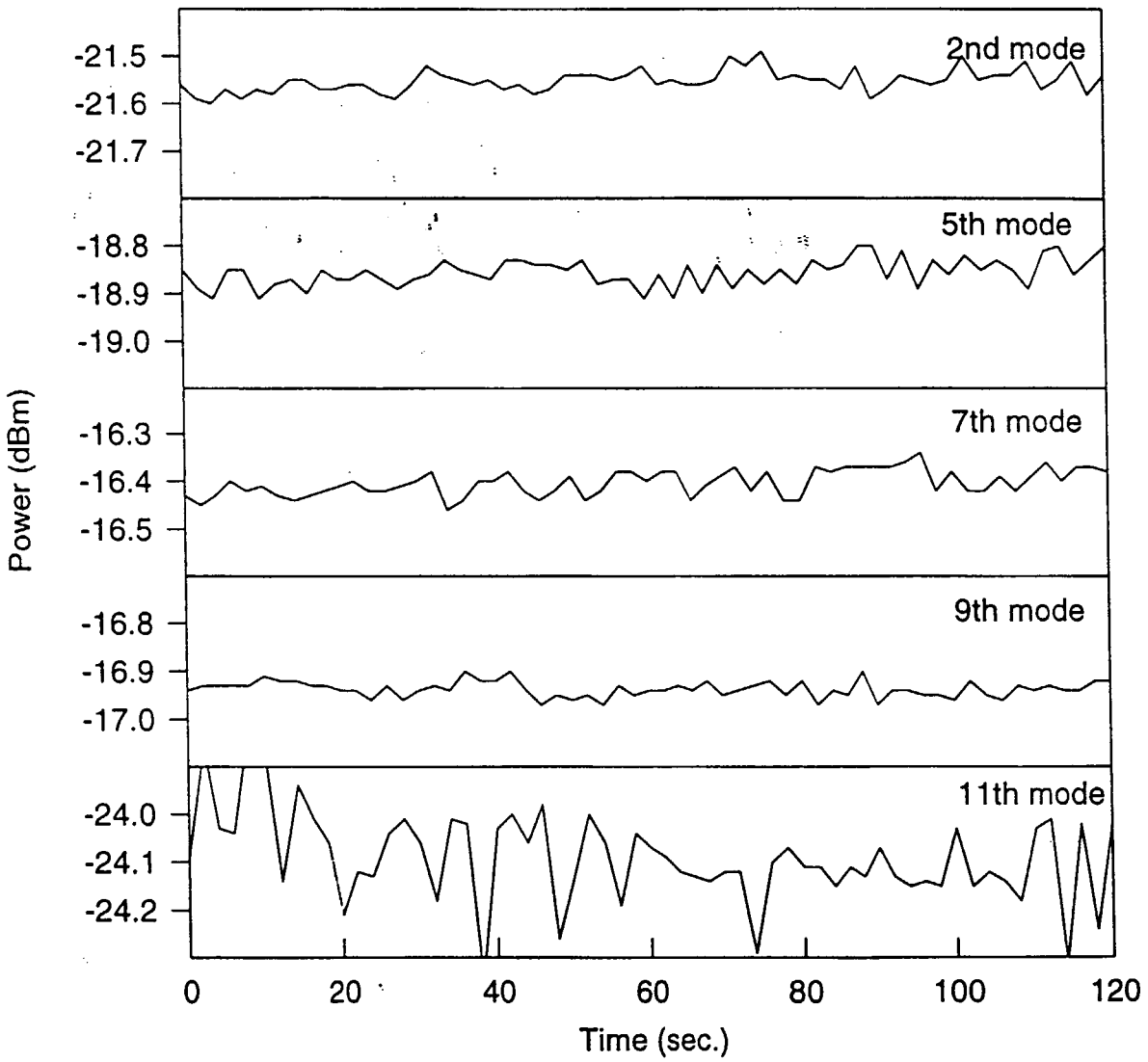
2nd mode
5th mode
7th mode
9th mode
11th mode
-21.5
-21.6
-21.7
-18.8
-18.9
-19.0
-16.3
-16.4
-16.5
-16.8
-16.9
-17.0
-24.0
-24.1
-24.2
Power (dBm)
0
20
40
60
80
100
120
Time (sec.)

Figure 8 (b)

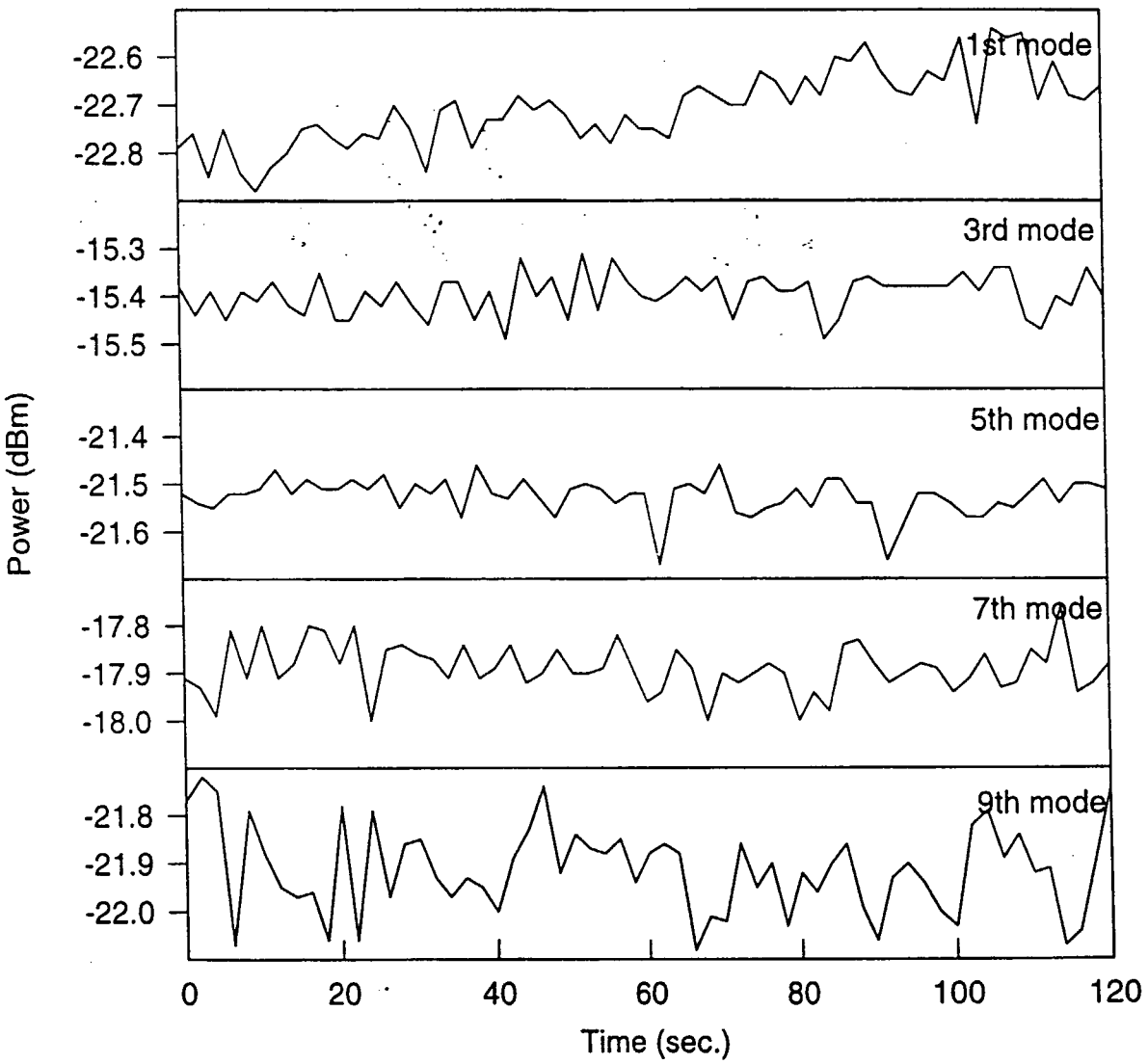
1st mode
3rd mode
5th mode
7th mode
9th mode
-22.6
-22.7
-22.8
-15.3
-15.4
-15.5
-21.4
-21.5
-21.6
-17.8
-17.9
-18.0
-21.8
-21.9
-22.0
Power (dBm)
0
20
40
60
80
100
120
Time (sec.)

Figure 8 (c)

S. Yamashita, et

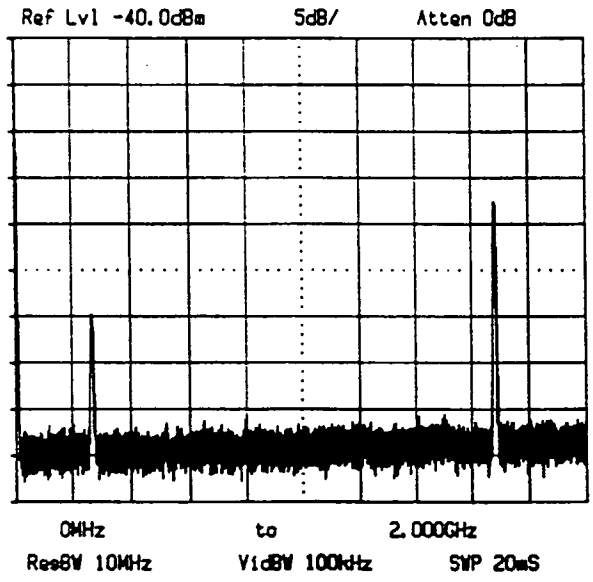

Figure 9

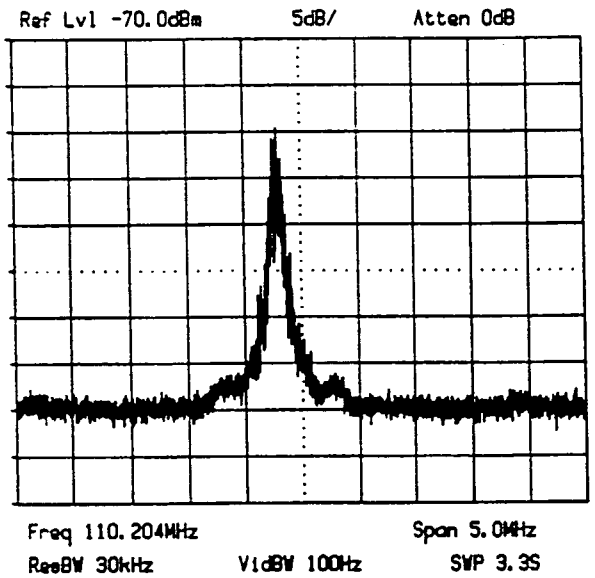
Ref Lvl -70.0dBm
5dB/
Atten 0dB
Freq 110.204MHz
Span 5.0MHz
ResBW 30kHz
VidBW 100Hz
SWP 3.3S

Figure 10

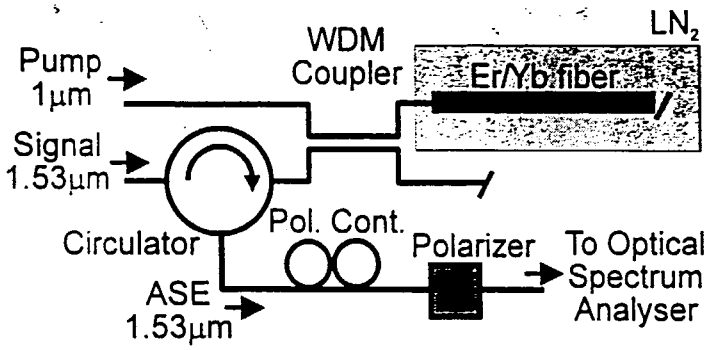
Pump
1μm
Signal
1.53μm
WDM
Coupler
LN2
Er/Yb fiber
Circulator
Pol. Cont.
Polarizer
To Optical
Spectrum
Analyser
ASE
1.53μm

Figure 11

S. Yamashita, et al.

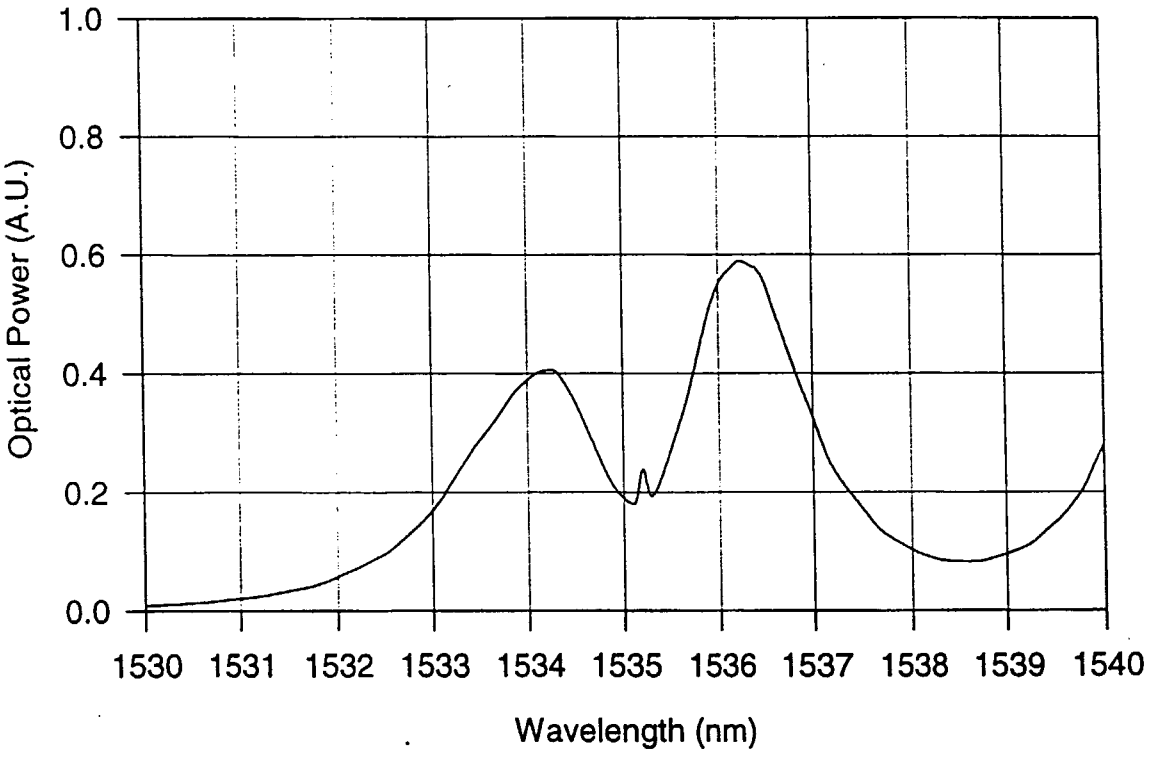

Figure 12(a)

S. Yamashita, et al.

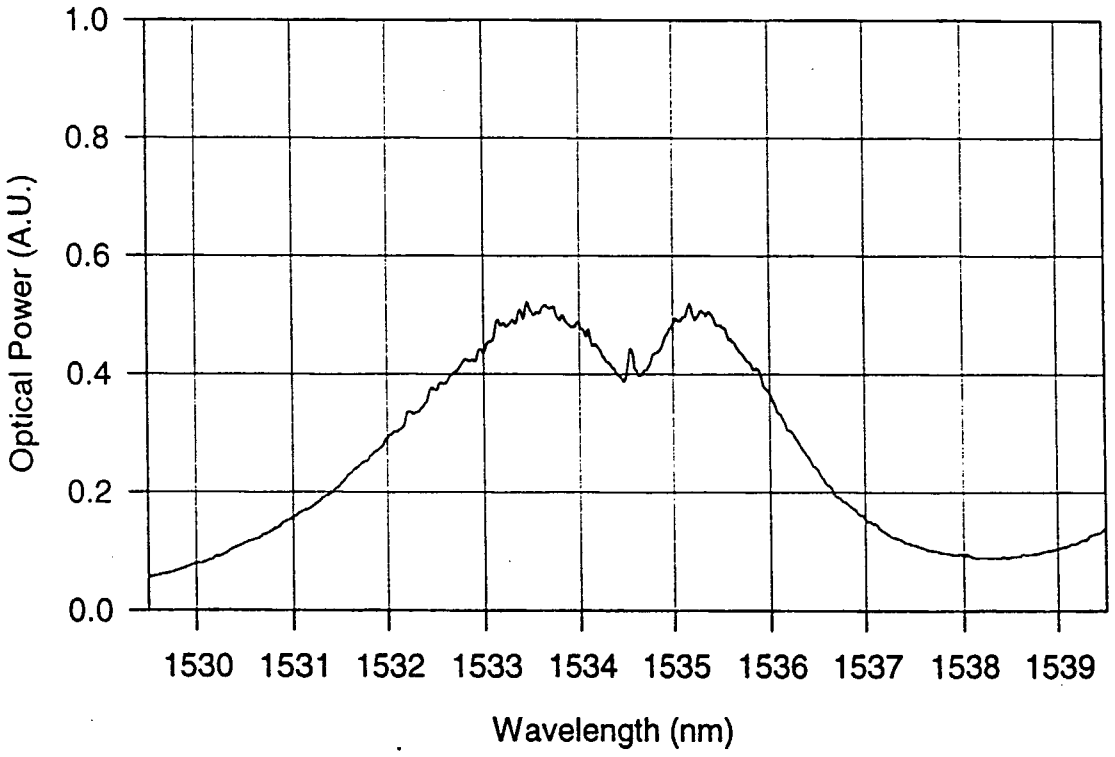

Figure 12(b)

S. Yamashita, et al

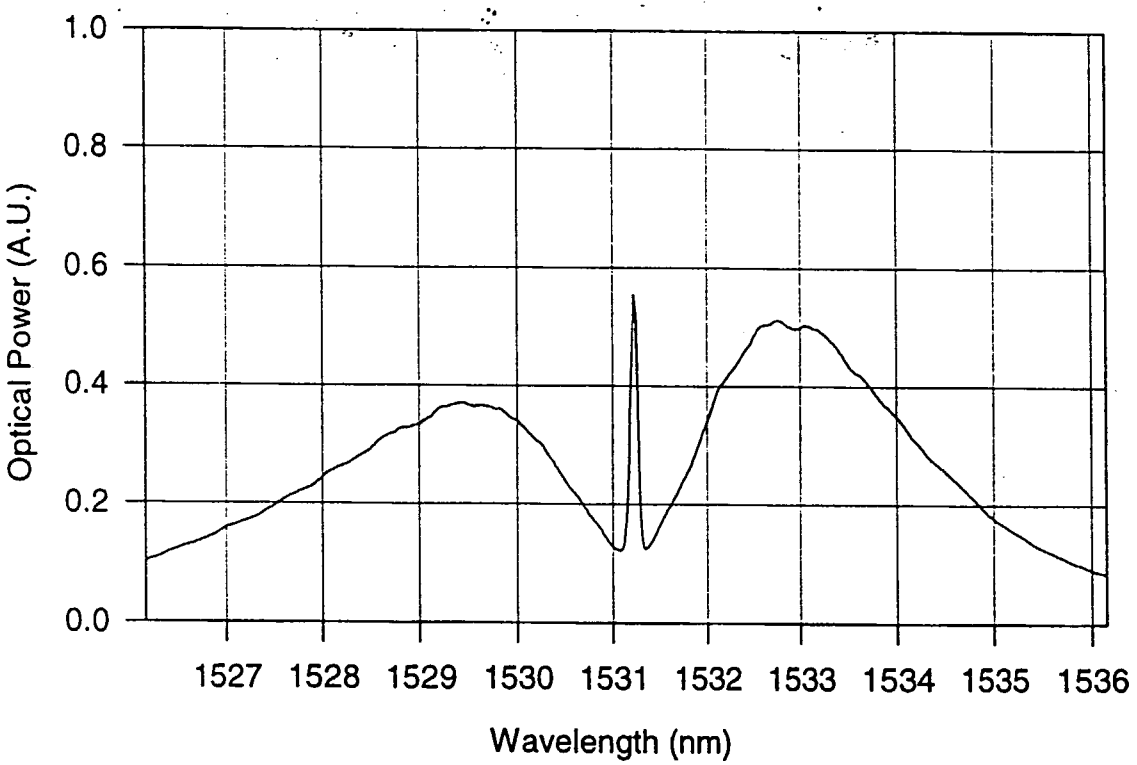

Figure 12(c)